Interplay of Substrate Surface Energy and Nanoparticle Concentration in Suppressing Polymer Thin Film Dewetting

Sudeshna Roy,[1,2] Diya Bandyopadhyay,[2] Alamgir Karim,[2,3*] and Rabibrata Mukherjee[1*]
[1]Department of Chemical Engineering, IIT Kharagpur, 721302, India
[2]Department of Polymer Engineering, University of Akron, OH 44325, USA
[3]Akron Functional Materials Centre (AFMC), University of Akron, OH 44325, USA

Online Supporting Information

1.0 Measurement of Substrate Surface Energy and Calculation of Interfacial Energies between Different Components

Contact angle (CA) measurement shows that the substrate surface energy (γ_S) varies with progressive UVO exposure. The magnitude of γ_S after different durations of UVO is calculated using the Young Dupre Equation (E–1), given below.

$$\boldsymbol{\gamma_L(\cos\theta + 1) = 2\left[\sqrt{\gamma_S^{LW}\gamma_L^{LW}} + \sqrt{\gamma_S^{+}\gamma_L^{-}} + \sqrt{\gamma_S^{-}\gamma_L^{+}}\right]} \quad \text{(E1) (Equation 41 of Reference No. 1)}$$

The unknowns are γ_S^{LW}, γ_S^{+} and γ_S^{-}. In order to evaluate these three unknowns, three probing liquids are necessary, which were Water, Ethylene Glycol and Toluene. The surface tension components of the probing liquids as well as that of PS and C_{60} are given in Table S1.[2,3] Further, the interfacial energy between the substrate and PS (γ_{S-PS}), the substrate and the particles (γ_{S-C60}) and the particles and PS ((γ_{C60-PS}) are calculated using the Equation E2:

$$\boldsymbol{\gamma_{12} = \gamma_{12}^{LW} + \gamma_{12}^{P}} \quad \text{(E2)}$$

Where, $\boldsymbol{\gamma_{12}^{LW}}$ is the van der Waal's component of interfacial energy and $\boldsymbol{\gamma_{12}^{P}}$ is the Polar component of interfacial energy. The two components can be determined using the following equations:

$$\boldsymbol{\gamma_{12}^{LW} = \left(\sqrt{\gamma_1^{LW}} - \sqrt{\gamma_2^{LW}}\right)^2} \quad \text{(E3A)}$$

$$\boldsymbol{\gamma_{12}^{P} = 2\left(\sqrt{\gamma_1^{+}\gamma_1^{-}} + \sqrt{\gamma_2^{-}\gamma_2^{+}} - \sqrt{\gamma_1^{+}\gamma_2^{-}} - \sqrt{\gamma_1^{-}\gamma_2^{+}}\right)} \quad \text{(E3B)}$$

Also, $\boldsymbol{\gamma_1^{P} = 2\left(\sqrt{\gamma_1^{+}\gamma_1^{-}}\right)}$ (E3C)

Combining equation E2 with equations E3A and E3B, one obtains

$$\boldsymbol{\gamma_{12} = \gamma_1 + \gamma_2 - 2\left(\sqrt{\gamma_1^{LW}\gamma_2^{LW}} + \sqrt{\gamma_1^{+}\gamma_2^{-}} + \sqrt{\gamma_1^{-}\gamma_2^{+}}\right)} \quad \text{(E4) (Equation 43b of Reference No. 1)}$$

Table S1: Surface Tension components of the Probing Liquids used as well as PS and Fullerene (in mJ/m^2)

Name	**Molecular Formula**	**Surface Tension (mJ/m^2) @ 20°C**				
		Total (γ)	**Dispersive** (γ^{LW})	**Polar** (γ^{P})	**Acid** (γ^{+})	**Base** (γ^{-})
Water	H_2O	72.8	21.8	51	25.5	25.5
Ethylene Glycol	$C_2H_6O_2$	48	29	19	1.92/3	47/30.1
Toluene	C_7H_8	27.9	25.6	2.3	1.0	2.3
Polystyrene	$(C_8H_8)_n$	42.1	42.1	0	0	1.1
Fullerene	C_{60}	41.7	36.8	4.85	1	5.91

The variation of γ_S as a function of UVO exposure time (t_E) is shown in graphically shown in Figure S1. The measured values of contact angles with the three probing liquids on substrates exposed for different durations of UVO as well as the calculated values of γ_S^{LW}, γ_S^{+}, γ_S^{-} are listed in Table S2. The values of the interfacial tension between the different components are also listed there.

Table S2: Measured Contact Angle on substrates with different probing liquids,calculated substrate Surface Energy γ_S along with its components and Interfacial Energies γ_{S-C60} and γ_{S-PS} as a function of t_E.

	Measured Contact Angle (°)			**Calculated Surface Energy (Components/ Total) in mJ/m^2**						
t_E (min)	**Water** θ_W	**EG** θ_{EG}	**Toluene** θ_T	γ_S^{LW}	γ_S^{+}	γ_S^{-}	γ_S^{P}	γ_S	$\gamma_{S-C_{60}}$	γ_{S-PS}
0	85.8	62.3	3.0	24.61	0.52	5.87	3.47	**28.08**	1.287	5.962
2	74.7	48.5	3.0	20.42	2.56	11.02	10.62	**31.05**	3.524	14.557
4	56.4	37.2	3.0	15.61	4.33	29.84	22.74	**38.35**	11.069	29.179
6	49.8	31.2	3.0	14.15	5.35	36.83	28.09	**42.31**	14.909	35.525
8	41.2	26.3	3.0	12.66	6.03	47.43	33.82	**46.53**	19.278	42.375
10	32.5	19.8	3.0	11.41	6.83	56.99	39.47	**50.88**	23.786	49.146
12	27.3	17.4	3.0	10.86	7.04	62.58	42.02	**52.87**	25.846	52.193
15	24.3	14.3	3.0	10.55	7.35	65.01	43.73	**54.28**	27.260	54.203
17	18.6	10.2	2.0	10.10	7.62	69.75	46.13	**56.23**	29.178	56.996
20	3.0	3.0	2.0	9.53	7.85	76.54	49.05	**58.50**	31.697	60.618
30	3.0	3.0	2.0	9.53	7.85	76.54	49.05	**58.50**	31.697	60.618

γ_{C60-PS} **= 5.078 mJ/m^2**

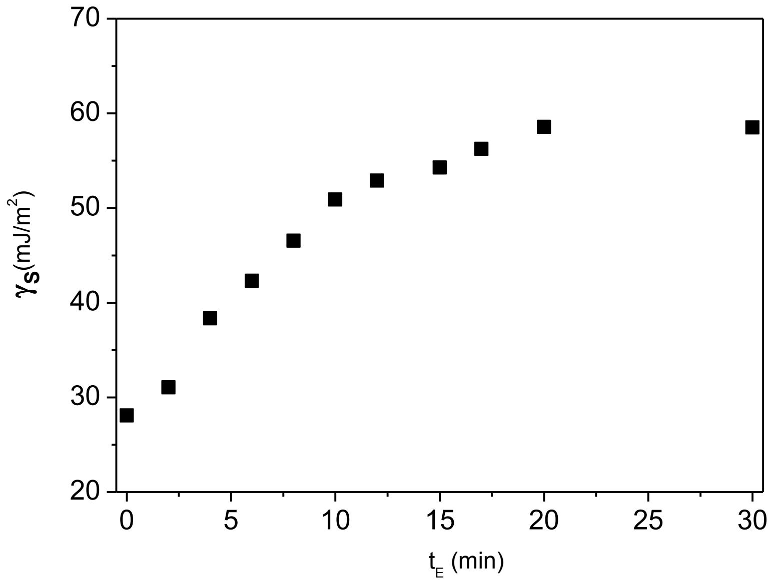

Figure S1: *Plot of Surface Energy of the substrate vs. UVO exposure time (**t_E**).*

Free Energy of Adhesion ($\Delta G_{C60\text{-}PS\text{-}S}$)

Based on the above data we calculated the Free Energy of Adhesion ($\Delta G_{C60\text{-}PS\text{-}S}$), which indicates the change in free energy when C60 (particles) and the substrate comes in contact with each other by displacing a layer of PS between them. This can be calculated as per the following formulae: $\Delta G_{C60\text{-}PS\text{-}S} = \gamma_{S-C_{60}} - (\gamma_{S-PS} + \gamma_{C60-PS})$ (E5)

A negative value of $\Delta G_{C60\text{-}PS\text{-}S}$ indicates attachment of the particles and the substrate and lower is the value; more favored will be the adhesion. Table S3 gives the value of $\Delta G_{C60\text{-}PS\text{-}S}$ as a function of γ_s

γ_s *(mJ/m^2)*	$\Delta G_{C60\text{-}PS\text{-}S}$ *(mJ/m^2)*
28.08	- 2.171
31.05	-13.003
38.35	- 35.170
42.31	- 45.356
46.53	- 56.575
50.88	- 67.854
52.87	-72.961
54.28	- 76.385
56.23	- 81.096
58.50	- 87.237

2.0 Morphology of as Cast Films (Particle Free as well as Particle Containing)

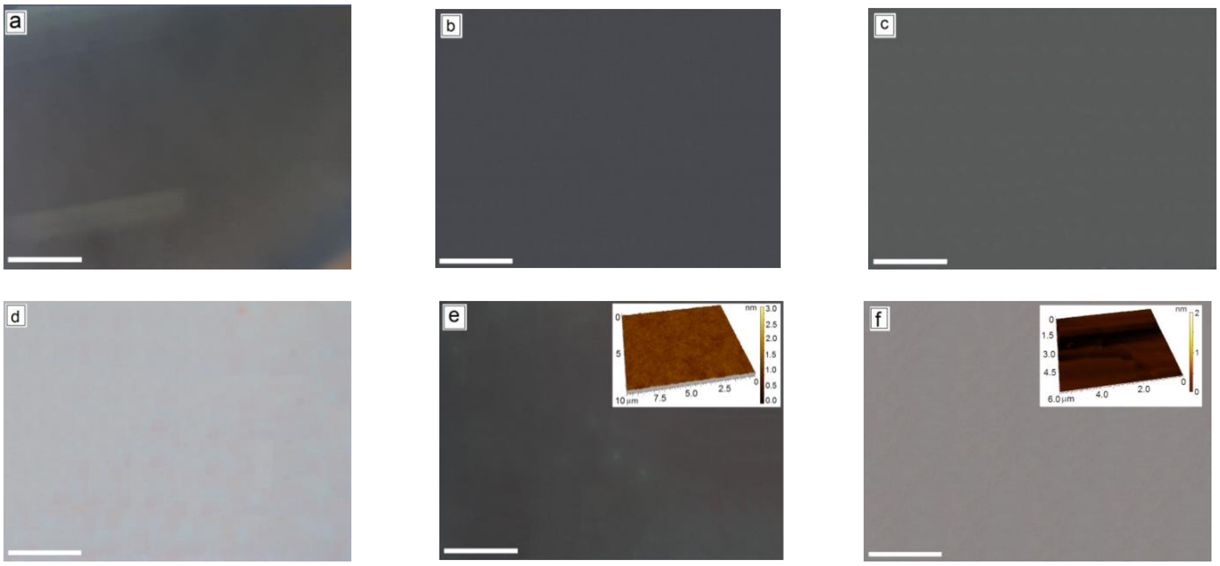

Figure S2: *Optical Microscope images of as cast films prior to annealing.(a) particle free on a substrate with γ_S = 28.04 mJ/m^2; (b) C_{NP} = 0.1% on a substrate with γ_S = 28.04 mJ/m^2; (c) C_{NP} = 0.1 % on a substrate with γ_S = 58.50 mJ/m^2; (d) C_{NP} = 0.625 % on a substrate with γ_S = 58.50 mJ/m^2. (e) C_{NP} = 1.0 % on a substrate having γ_S = 28.04 mJ/m^2; (f) C_{NP} = 1.0 % on a substrate having γ_S = 58.50 mJ/m2. Scale bar is 100 μm in all the cases. Inset to frames e and f shows the AFM scan of the film surface, and the very low surface roughness.*

Interfacial Morphology of the as Cast Films after Peeling the Film

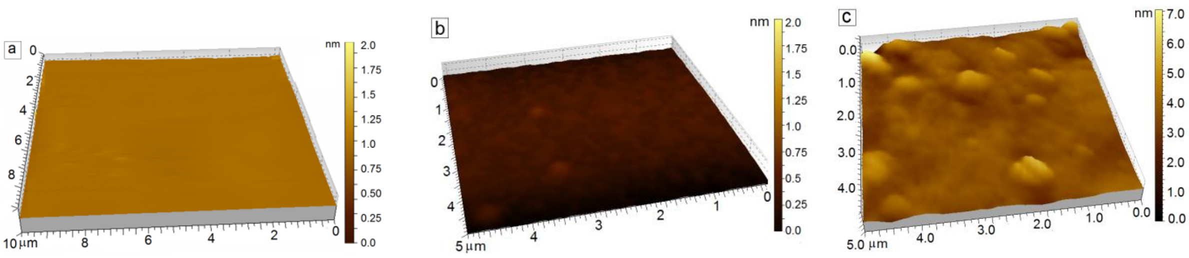

Figure S3: *Morphology of the film – substrate interface of the as cast films. (a) Particle free film on a substrate with γ_S = 58.50 mJ/m^2, (b) film with $\mathbf{C_{NP}}$ = 0.5% on a substrate with γ_S = 58.50 mJ/m^2, and (c) film with $\mathbf{C_{NP}}$ = 2.0 % on a substrate with γ_S = 58.50 mJ/m^2.*

3.0 Morphology of Dewetted Films

Morphology of Dewetted Films with no particles (C_{NP} = 0.0%) (Control Experiment)

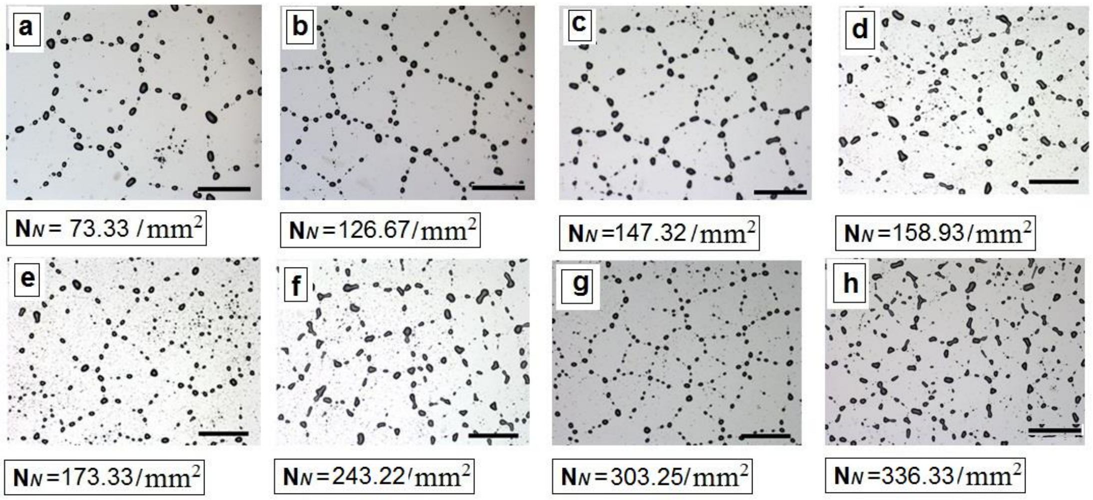

Figure S4: *Optical Microscopy images of completely dewetted 112 nm thick particle free films, annealed for 46 hours at 130°C. The surface energy of the substrate is: (a) 28.04, (b) 31.05, (c) 38.35, (d) 42.31, (e) 46.53, (f) 50.88, (g) 54.28, and (h) 58.50 mJ/m^2. Scale bar = 100 μm.*

3.1 Morphology of Fully Dewetted Particle Containing Films (Regime 1)

C_{NP} = 0.1% (Regime 1, Complete Dewetting)

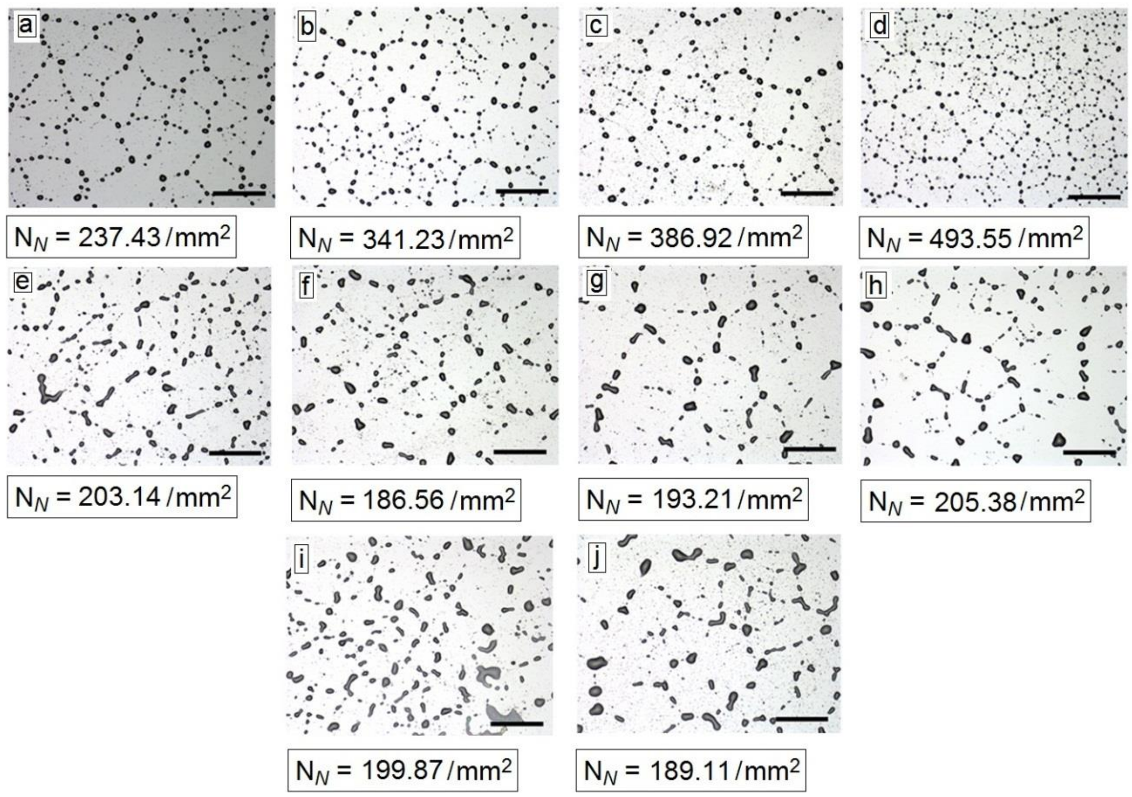

Figure S5: *Optical Microscopy images of completely dewetted 112 nm thick films with **C_{NP}** = 0.1 %, annealed for 46 hours at 130°C. The surface energy (mJ/m^2) of the substrate is: (a) 28.08, (b) 31.05, (c) 38.35, (d) 42.31, (e) 46.53, (f) 50.88, (g) 52.87, (h) 54.28, (i) 56.23 and (j) 58.50. Scale bar = 100 μm.*

C_{NP} = 0.2%   (Regime 1, Complete Dewetting)

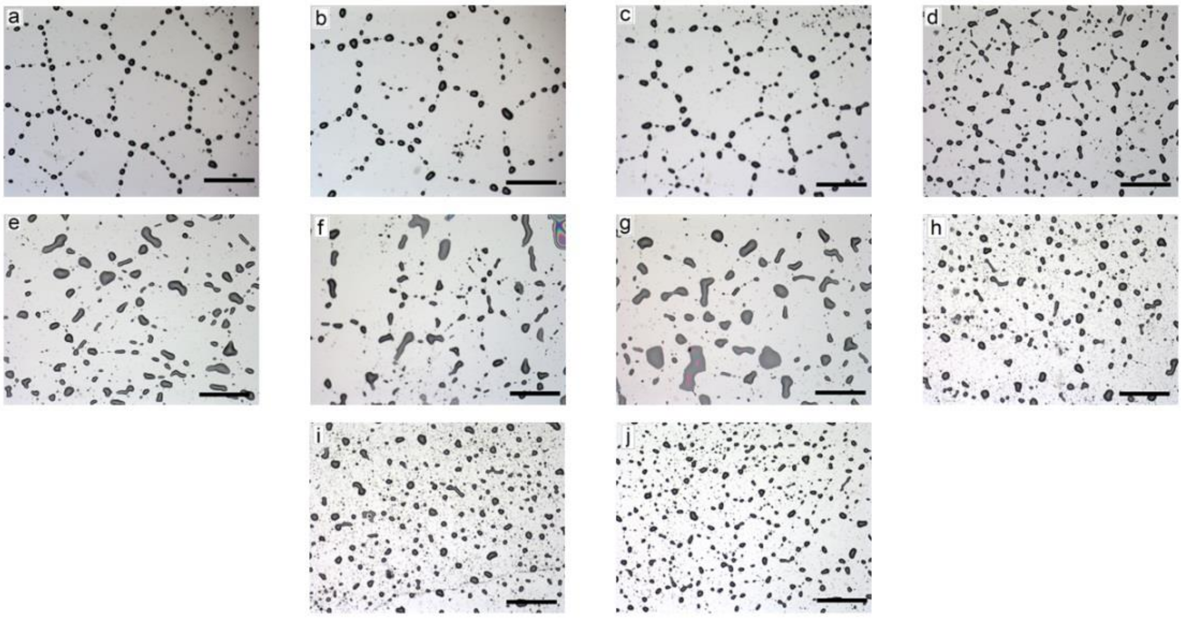

Figure S6: *Optical Microscopy images of completely dewetted 112 nm thick films with* $\boldsymbol{C_{NP}}$ *= 0.2 %, annealed for 46 hours at 130°C. The surface energy (mJ/m*^{2}*) of the substrate is: (a) 28.08, (b) 31.05, (c) 38.35, (d) 42.31, (e) 46.53, (f) 50.88, (g) 52.87, (h) 54.28, (i) 56.23 and (j) 58.50. Scale bar = 100* μ*m.*

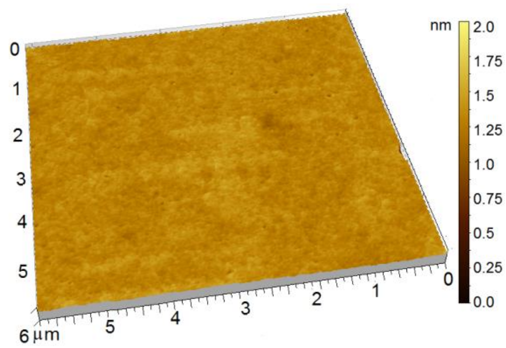

Figure S7: *Particle free smooth substrate – film interface after 46 hours of annealing, in a film with* $\boldsymbol{C_{NP}}$ *= 0.1 % on a substrate with* $\boldsymbol{\gamma_S}$ *= 31.05 mJ/m*^{2}*.*

3.2 Morphology of Partially Dewetted Particle Containing Films (Regime 2)

C_{NP} = 0.3 %   (Regime2, Partial Dewetting)

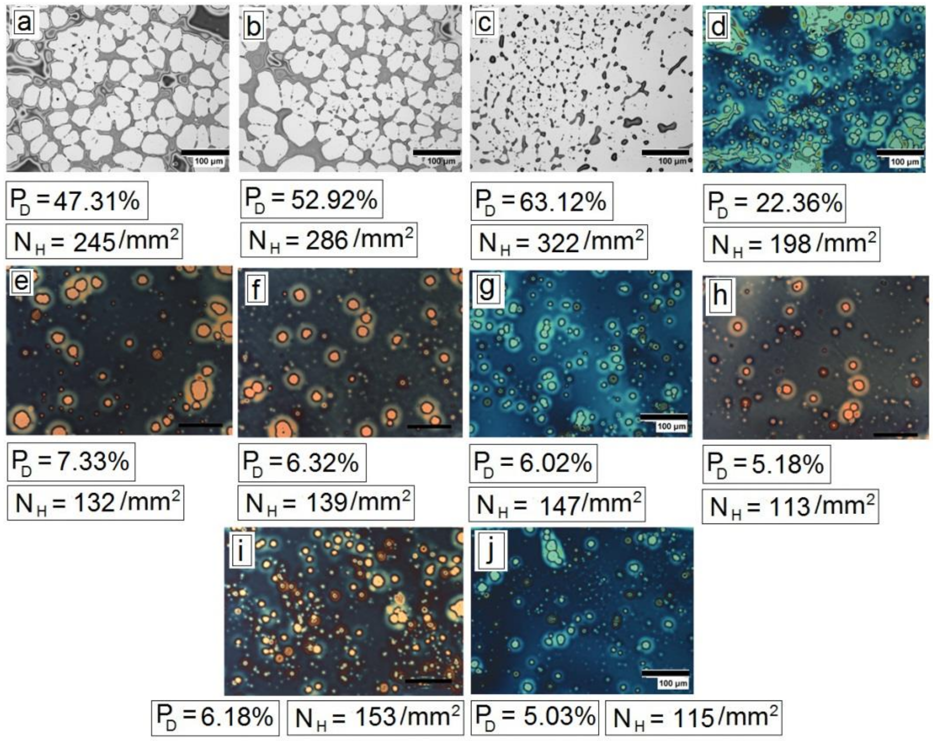

Figure S8: *Optical Microscopy images of partially dewetted 112 nm thick films with* $\boldsymbol{C_{NP}}$ *= 0.3 %, annealed for 46 hours at 130°C. The surface energy (mJ/m^2) of the substrate is: (a) 28.08, (b) 31.05, (c) 38.35, (d) 42.31, (e) 46.53, (f) 50.88, (g) 52.87, (h) 54.28, (i) 56.23 and (j) 58.50. Scale bar = 100 μm.*

C_{NP} = 0.5 %   (Regime2, Partial Dewetting)

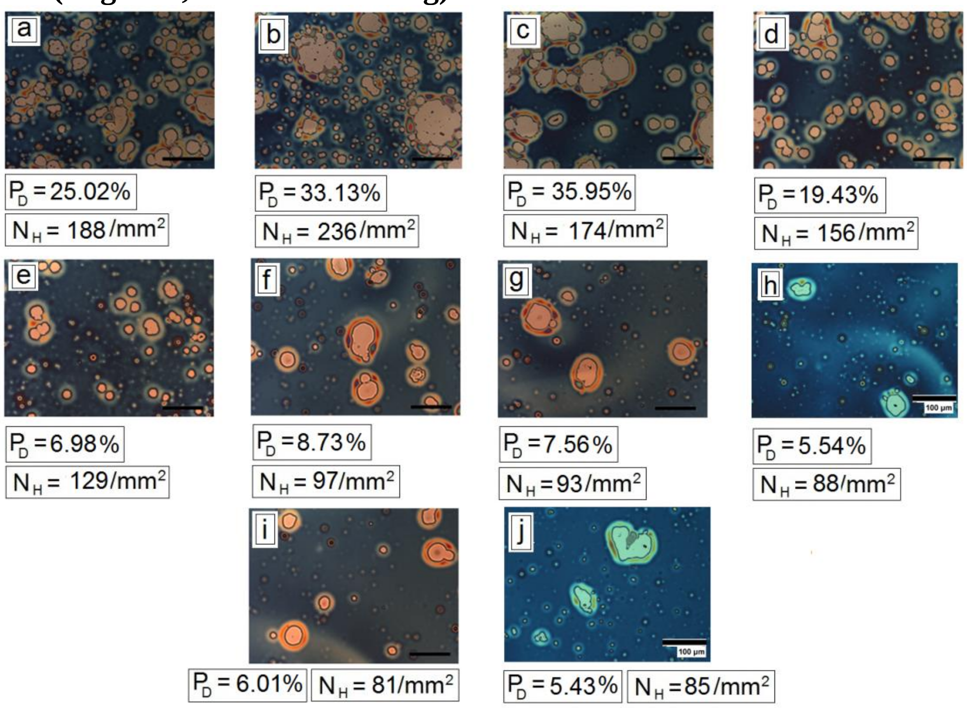

Figure S9: *Optical Microscopy images of partially dewetted 112 nm thick films with* $\boldsymbol{C_{NP}}$ *= 0.5 %, annealed for 46 hours at 130°C. The surface energy (mJ/m^2) of the substrate is: (a) 28.08, (b) 31.05, (c) 38.35, (d) 42.31, (e) 46.53, (f) 50.88, (g) 52.87, (h) 54.28, (i) 56.23 and (j) 58.50. Scale bar = 100 μm.*

C_{NP} = 0.625 % **(Regime2, Partial Dewetting)**

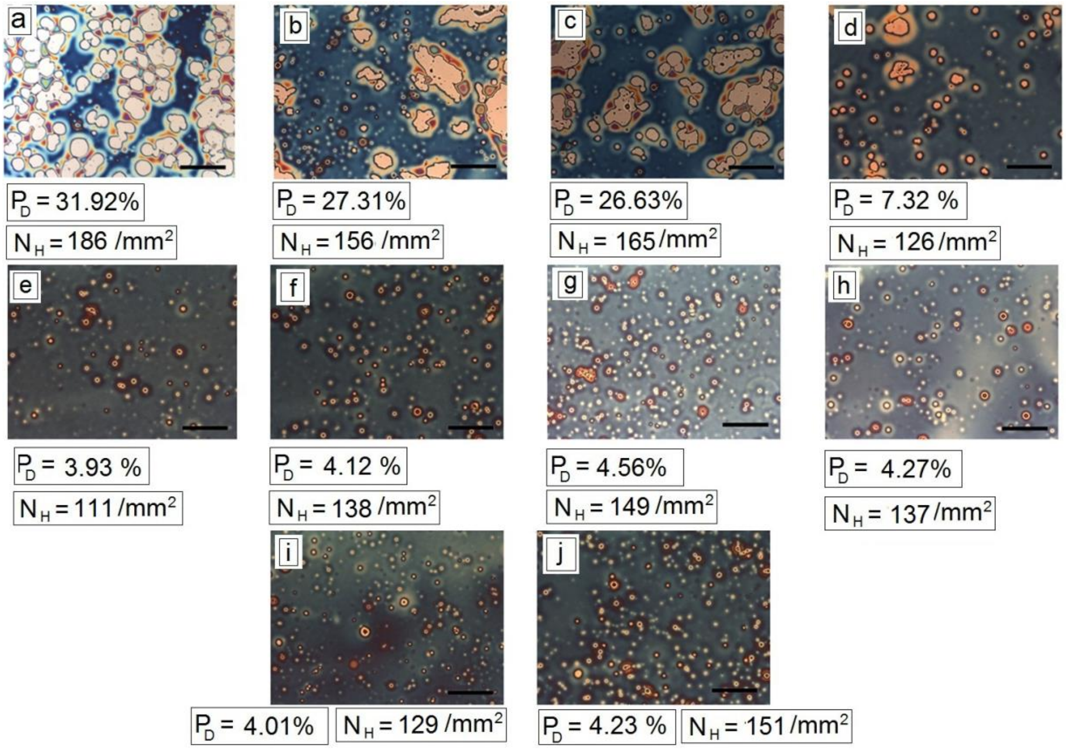

Figure S10: *Optical Microscopy images of partially dewetted 112 nm thick films with* $\boldsymbol{C_{NP}}$ *= 0.625 % annealed for 46 hours at 130°C. The surface energy (mJ/m^2) of the substrate is: (a) 28.08, (b) 31.05, (c) 38.35, (d) 42.31, (e) 46.53, (f) 50.88, (g) 52.87, (h) 54.28, (i) 56.23 and (j) 58.50. Scale bar = 100 μm. The % of dewetting (*$\boldsymbol{P_D}$*) and the Number density of holes (*$\boldsymbol{N_H}$*) are marked in each frame.*

C_{NP} = 0.75 % (Regime2, Partial Dewetting)

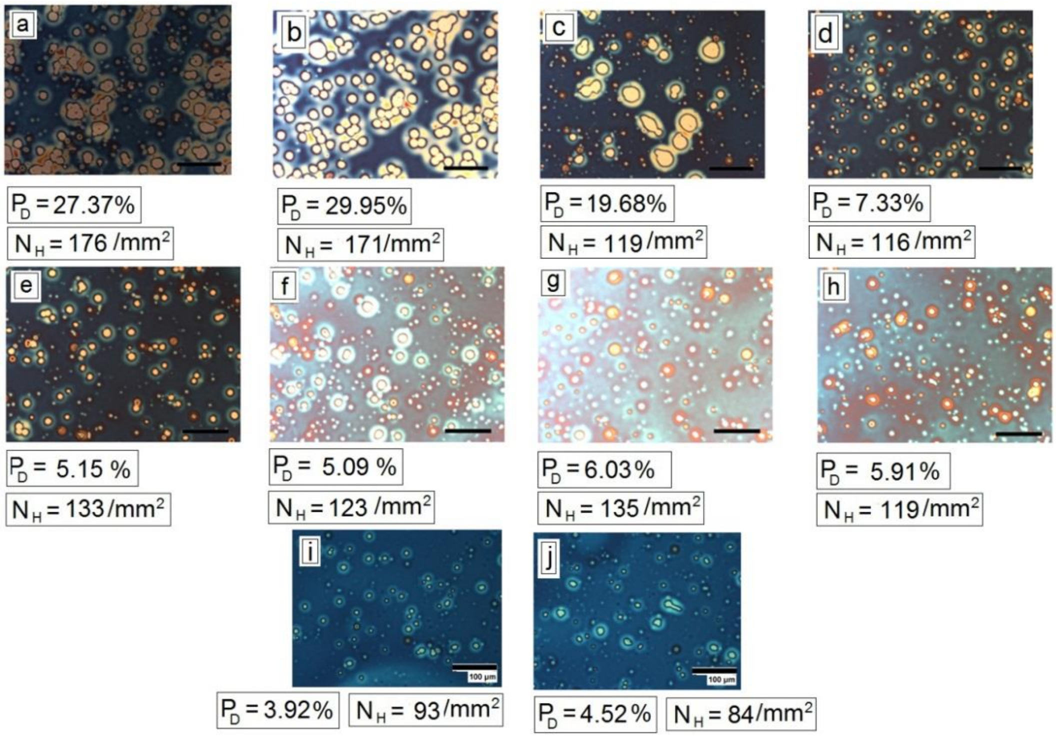

Figure S11: *Optical Microscopy images of partially dewetted 112 nm thick films with* $\boldsymbol{C_{NP}}$ *= 0.75 %, annealed for 46 hours at 130°C. The surface energy (mJ/m^2) of the substrate is: (a) 28.08, (b) 31.05, (c) 38.35, (d) 42.31, (e) 46.53, (f) 50.88, (g) 52.87, (h) 54.28, (i) 56.23 and (j) 58.50. Scale bar = 100 μm.*

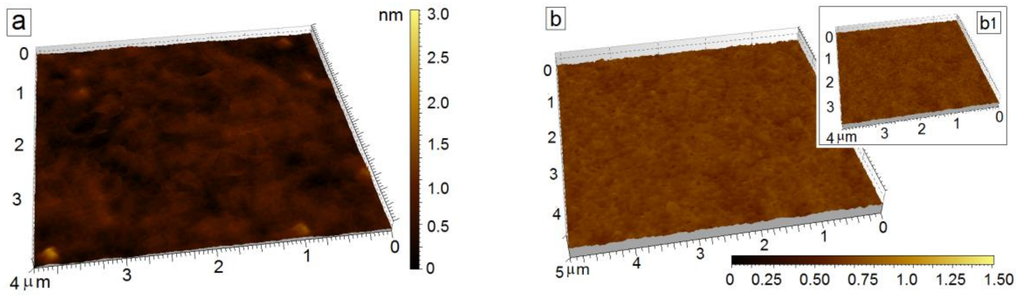

Figure S12: *Morphology of the substrate – film interface after 46 hours of annealing, in a film with* $\boldsymbol{C_{NP}}$ *= 0.625 %. (a) The interface is smooth and free from any particle cluster on a substrate with* $\boldsymbol{\gamma_S}$ *= 28.08 mJ/m*^{2} *and (b) 38.35 mJ/m*^{2}*.*

3.3 Morphology of Completely stable Particle Containing Films (Regime 3)

C_{NP} = 1.0%   (Regime 3, Complete Suppression of Dewetting)

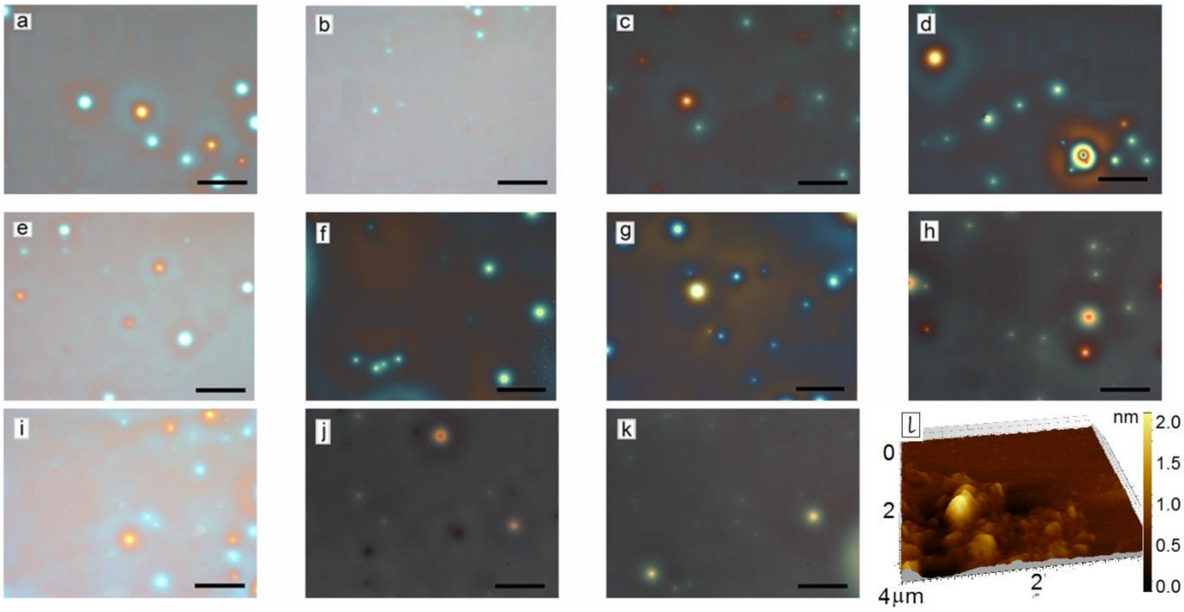

Figure S13: *Optical Microscopy images of 112 nm thick films with* $\boldsymbol{C_{NP}}$ *= 1.0%, annealed for 46 hours at 130°C, with no sign of dewetting. The surface energy (mJ/m*^{2}*) of the substrate is: (a) 28.08, (b) 31.05, (c) 38.35, (d) 42.31, (e) 46.53, (f) 50.88, (g) 52.87, (h) 54.28, (i) 56.23, (j) 58.50 and (k) 58.50. Scale bar = 100* μ*m. (l) Typical AFM morphology of the tiny clusters formed on the film surface.*

C_{NP} = 2.0%   (Regime 3, Complete Suppression of Dewetting)

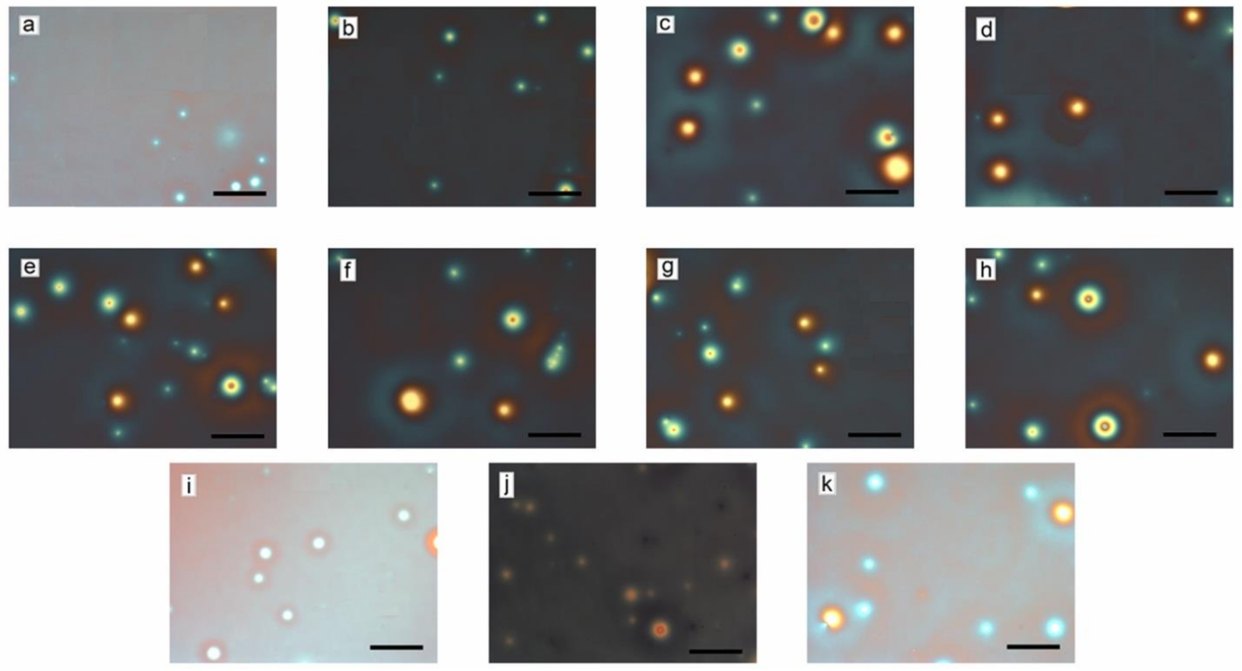

Figure S14: *Optical Microscopy images of 112 nm thick films with* ***C_{NP}*** *=2.0%, annealed for 46 hours at 130°C, with no sign of dewetting. The surface energy (mJ/m^2) of the substrate is: (a) 28.08, (b) 31.05, (c) 38.35, (d) 42.31, (e) 46.53, (f) 50.88, (g) 52.87, (h) 54.28, (i) 56.23, (j) 58.50 and (k) 58.50. Scale bar = 100 μm. The white spots are particle clusters formed during spin coating itself, which can be seen in inset to figure 1c.*

4.0 Calculation of $\chi_{PS-C_{60}}$:

Compiled values of PS and C_{60} solubility parameter:

δ_{PS} **:**

1. 17.9±0.2 $MPa^{1/2}$ (Ref 4)
2. 18.6 $MPa^{1/2}$ (Ref 5,6)
3. 17.5-19.1 $MPa^{1/2}$ (Ref 7)
4. 9.1 $(cal/cm^3)^{1/2}$ (Ref 8 – 10) ≈ 18.6 $MPa^{1/2}$
5. 7.6±0.2 $(cal/cm^3)^{1/2}$ at 193 °C (Ref 11)
6. 18.5 $MPa^{1/2}$ (Ref 12)

$\delta_{C_{60}}$ **:**

1. 20.09 $MPa^{1/2}$ (Ref 13,14)
2. 18.5 $MPa^{1/2}$ (Ref 15)
3. 9.8 $(cal/cm^3)^{1/2}$ (Ref 16)

4.1 Calculated chi value:

Sl. No.	δ_{PS}	$\delta_{C_{60}}$	$\chi_{PS-C_{60}}$
1.	18.1	20.09	0.1745
2.	18.1	18.5	0.007
3.	18.1	20.046	0.167
4.	17.7	20.09	0.252
5.	17.7	18.5	0.028
6.	17.7	20.046	0.242
7.	18.6	20.09	0.0984
8.	18.6	18.5	0.00044
9.	18.6	20.046	0.092
10.	17.5	20.09	0.2955
11.	17.5	18.5	0.044
12.	17.5	20.046	0.2856
13.	19.1	20.09	0.043
14.	19.1	18.5	0.016
15.	19.1	20.046	0.039
16.	18.5	20.09	0.1114
17.	18.5	18.5	0
18.	18.5	20.046	0.1053
19.	15.955	20.09	0.441 (at 193 °C)
20.	15.955	18.5	0.167 (at 193 °C)
21.	15.955	20.046	0.432 (at 193 °C)
22.	15.136	20.09	0.633 (at 193 °C)
23.	15.136	18.5	0.292 (at 193 °C)
24.	15.136	20.046	0.622 (at 193 °C)

4.2 Sample Calculation of $\chi_{PS-C_{60}}$:

It is calculated using regular solution theory as described by Emerson *et al.*[4]

$$\chi_{PS-C_{60}} = \frac{V_0}{RT}\left(\delta_{PS} - \delta_{C_{60}}\right)^2$$

$\chi_{PS-C_{60}}$ is the polymer-polymer interaction parameter

V_0 is the geometric mean of polymer segment molar volumes (for simplicity of calculation it is taken as 100 cm^3/mol)

R is the gas constant (R= 8.314 J/mol.K)

T is the temperature in temperature in K (T=273 K)

δ_{PS} and $\delta_{C_{60}}$ are the solubility parameter of PS and C_{60} respectively.[5,6]

δ_{PS} = 18.6 $MPa^{1/2}$

$\delta_{C_{60}}$ = 20.09 $MPa^{1/2}$

Calculated interaction parameter of PS-C_{60}: $\chi_{PS-C_{60}}$ = 0.0984

References:

1. Van Oss, C. J.; Chaudhury, M. K.; Good, R. J. *Chem. Rev.* **1988**, *88*, 927-941
2. Cwikel, D.; Zhao, Q.; Liu, C.; Su, X.; Marmur, A. *Langmuir* **2010**, *26*, 15289-15294.
3. Ma, X.; Wigington, B.; Bouchard, D. *Langmuir* **2010**, *26*, 11886-11893.
4. Emerson, J. A.; Toolan, D. T. W.; Howse, J. R.; Furst, E. M.; Epps, T. H. *Macromolecules* **2013**, *46*, 6533–6540.
5. Gong, Y.; Huang, H.; Hu, Z.; Chen, Y.; Chen, D.; Wang, Z.; He, T. *Macromolecules* **2006**, *39*, 3369–3376.
6. Jang, B. N.; Wang, D.; Wilkie, C. A. *Macromolecules* **2005**, *38*, 6533–6543.
7. Price, A. D.; Hur, S.; Fredrickson, G. H.; Frischknecht, A. L.; Huber, D. L. *Macromolecules* **2012**, *45*, 510–524.
8. Dekeyser, C. M.; Biltresse, S.; Marchand-brynaert, J.; Rouxhet, P. G.; Dupont-gillain, C. C. *Polymer* **2004**, *45*, 2211–2219.
9. Blanks, R. F.; Prausnitz, J. M. *IEC Fundamentals* **1964**, *2*, 1–8.
10. Weng, H.; Huang, X.; Wang, M.; Ji, X.; Ge, X. *Langmuir* **2013**, *29*, 15367–15374.
11. Guillet, E.; September, R. *Macromolecules* **1978**, *1*, 228–235.

12. Gotrik, K. W.; Hannon, A. F.; Son, J. G.; Keller, B.; Alexander-Katz, A.; Ross, C. A. *ACS Nano* **2012**, *6*, 8052–8059.
13. Huang, J. *Fluid Phase Equilibr* **2005**, *237*, 186–192.
14. Hansen, C. M.; Smith, A. L. *Carbon* **2004**, *42*, 1591–1597.
15. Solvents, O. *J. Org. Chem* **1992**, *8*, 6077–6079.
16. Ruoff, R. S.; Tse, D. S.; Malhotra, R.; Lorents, D. C. *J. Phys. Chem.* **1993**, *97*, 3379–3383.